Title

Predicting Responses to Neoadjuvant Chemotherapy in Breast Cancer: ACRIN 6691 Trial of Diffuse Optical Spectroscopic Imaging

Journal

Cancer Research, 76(20)

ISSN

0008-5472

Authors

Tromberg, Bruce J

investigators, on behalf of the ACRIN 6691

Zhang, Zheng

et al.

Publication Date

2016-10-15

DOI

10.1158/0008-5472.can-16-0346

Peer reviewed

HHS Public Access

Author manuscript

Cancer Res. Author manuscript; available in PMC 2017 October 15.

Published in final edited form as:

Cancer Res. 2016 October 15; 76(20): 5933–5944. doi:10.1158/0008-5472.CAN-16-0346.

Predicting Responses to Neoadjuvant Chemotherapy in Breast Cancer: ACRIN 6691 Trial of Diffuse Optical Spectroscopic Imaging (DOSI)

Bruce J. Tromberg[1,*], **Zheng Zhang**[2], **Anaïs Leproux**[1], **Thomas D. O'Sullivan**[1], **Albert E. Cerussi**[1], **Philip Carpenter**[3], **Rita S. Mehta**[4], **Darren Roblyer**[5], **Wei Yang**[6], **Keith D. Paulsen**[7], **Brian W. Pogue**[7], **Shudong Jiang**[7], **Peter Kaufman**[8], **Arjun G. Yodh AG**[9], **So Hyun Chung**[9], **Mitchell Schnall**[10], **Bradley S. Snyder**[11], **Nola Hylton**[12], **David A. Boas**[13], **Stefan A. Carp**[13], **Steven J. Isakoff**[14], and **David Mankoff**[15] **on behalf of the ACRIN 6691 investigators**

Bruce J. Tromberg: bjtrombe@uci.edu; Zheng Zhang: zzhang@stat.brown.edu; Anaïs Leproux: aleproux@uci.edu; Thomas D. O'Sullivan: tosulliv@uci.edu; Albert E. Cerussi: acerussi@gmail.com; Philip Carpenter: Philip.Carpenter@med.usc.edu; Rita S. Mehta: rsmehta@uci.edu; Darren Roblyer: roblyer@bu.edu; Wei Yang: wyang@mdanderson.org; Keith D. Paulsen: Keith.D.Paulsen@dartmouth.edu; Brian W. Pogue: Brian.W.Pogue@dartmouth.edu; Shudong Jiang: shudong.jiang@dartmouth.edu; Peter Kaufman: peter.a.kaufman@hitchcock.org; Arjun G. Yodh AG: yodh@physics.upenn.edu; So Hyun Chung: sophiechung12@gmail.com; Mitchell Schnall: Mitchell.Schnall@uphs.upenn.edu; Bradley S. Snyder: bsnyder@stat.brown.edu; Nola Hylton: Nola.Hylton@ucsf.edu; David A. Boas: dboas@nmr.mgh.harvard.edu; Stefan A. Carp: carp@nmr.mgh.harvard.edu; Steven J. Isakoff: SISAKOFF@mgh.harvard.edu; David Mankoff: David.Mankoff@uphs.upenn.edu

[1]Beckman Laser Institute and Medical Clinic, University of California Irvine

[2]Department of Biostatistics and Center for Statistical Sciences, Brown University School of Public Health

[3]Department of Pathology, University of Southern California

[4]Department of Medicine, University of California Irvine

[5]Department of Biomedical Engineering, Boston University

[6]Department of Radiology, MD Anderson Cancer Center

[7]Thayer School of Engineering, Dartmouth College

[8]Hematology and Oncology, Dartmouth-Hitchcock Medical Center

[9]Department of Physics and Astronomy, University of Pennsylvania

[10]Department of Radiology, University of Pennsylvania

[11]Center for Statistical Sciences, Brown University School of Public Health

[12]Department of Radiology, University of California, San Francisco

[*]Corresponding Author: Bruce J. Tromberg, Laser Microbeam and Medical Program (LAMMP), Beckman Laser Institute and Medical Clinic, University of California, Irvine, Irvine, CA, 92617. Phone 949 824-8705. bjtrombe@uci.edu.

Disclosure of Potential Conflicts of Interest: A. Cerussi and B.J. Tromberg report patents, which are owned by the University of California, that are related to the technology and analysis methods described in this study. The University of California has licensed diffuse optical spectroscopic imaging technology and analysis methods to LG, Inc. This research was completed without LG, Inc. participation, knowledge, or financial support and data were acquired and processed from patients by coauthors unaffiliated with this entity. The Institutional Review Board and Conflict of Interest Office of the University of California, Irvine, have reviewed both patent and corporate disclosures and did not find any concerns. No potential conflicts of interest were disclosed by the other authors.

[13]A. A. Martinos Center for Biomedical Imaging, Department of Radiology, Massachusetts General Hospital

[14]Hematology Oncology, Massachusetts General Hospital

[15]Division of Nuclear Medicine, University of Pennsylvania

Abstract

The prospective multi-center ACRIN 6691 trial was designed to evaluate whether changes from baseline to mid-therapy in a Diffuse Optical Spectroscopic Imaging (DOSI)-derived imaging endpoint, the Tissue Optical Index (TOI), predict pathologic complete response (pCR) in women undergoing breast cancer neoadjuvant chemotherapy (NAC). DOSI instruments were constructed at the University of California, Irvine and delivered to 6 institutions where 60 subjects with newly-diagnosed breast tumors (at least 2 cm in the longest dimension) were enrolled over a 2-year period. Bedside DOSI images of the tissue concentrations of deoxy-hemoglobin (ctHHb), oxy-hemoglobin ($ctHbO_2$), water (ctH_2O), lipid, and TOI (ctHHb × ctH_2O/lipid) were acquired on both breasts up to 4 times during NAC treatment: baseline, one-week, mid-point, and completion. Of the 34 subjects (mean age 48.4 ± 10.7 years) with complete, evaluable data from both normal and tumor-containing breast, 10 (29%) achieved pCR as determined by central pathology review. The percent change in tumor to normal TOI ratio ($\%TOI_{TN}$) from baseline to mid-therapy ranged from −82% to 321%, with a median of −36%. Using pCR as the reference standard and receiver-operating characteristic curve methodology, $\%TOI_{TN}$ AUC was 0.60 (95% CI 0.39 to 0.81). In the cohort of 17 patients with baseline tumor oxygen saturation ($\%StO_2$) greater than the 77% population median, $\%TOI_{TN}$ AUC improved to 0.83 (95% CI 0.63 to 1.00). We conclude that the combination of baseline functional properties and dynamic optical response shows promise for clinical outcome prediction.

Keywords

Functional imaging; metabolic imaging; near infrared spectroscopy; breast cancer; neoadjuvant chemotherapy

1. Introduction

Neoadjuvant chemotherapy (NAC), or preoperative systemic therapy, offers unique opportunities for patient care and cancer drug development [1]. In addition to improving breast tissue conservation and cosmetic outcome, NAC can cause down-staging of the pre-surgical tumor and reduce the required extent of axillary dissection [2]. Studies have shown that pathological complete response (pCR) predicts patient survival [3, 4], and the US Food and Drug Administration now allows use of the pCR endpoint to support accelerated approval of drugs for high-risk early-stage breast cancer [5]. Importantly, NAC enables tumor response and chemotherapy effectiveness to be assessed on an individual patient basis, allowing oncologists to optimize treatment strategy and improve patient outcome.

In current clinical practice, NAC response assessment is determined predominantly by serial physical examination, mammography and/or ultrasound. Yeh et.al. [6] showed that

palpation, mammography, ultrasound and magnetic resonance imaging (MRI) had 19%, 26%, 35%, and 71% agreement, respectively, with final pathological response. These and other studies have shown that anatomical changes in tumor presentation are not reliable predictors of final pathological state [7–9]. Functional measurements of tumors from contrast-enhanced MRI [10], magnetic resonance spectroscopy (MRS) [11, 12], and positron emission tomography (PET) [13, 14] have shown substantial improvement over conventional anatomic imaging. However, the cost, radiation exposure, and/or potential toxicities of contrast agents limit the frequency of these scans. Optical imaging offers a low-cost, risk-free approach that could be used as a “bedside” adjunct to these methods.

Currently, morphological criteria are the only clinical care standards for evaluating therapeutic efficacy of NAC. Prior studies have indicated that functional and molecular measures may provide an early indicator of breast cancer therapy response in the neo-adjuvant setting. Studies support the potential value of proliferation biomarkers, including imaging markers [15], as predictors of therapeutic response [16, 17]. Other imaging studies indicate that early changes in blood flow and tumor metabolism predict subsequent response and provide an early marker for cellular response to treatment [10–12, 18]. Taken together, evidence suggests that early (24 to 72 hours) tumor biochemical changes precede volumetric changes in response to cancer therapies [19, 20]. These early biochemical changes may provide a pathway for predicting final pathological outcome [20]. Early classification of therapeutic effectiveness could increase patient survival and minimize unnecessary damage to sensitive tissues (e.g. heart, liver, brain) caused by ineffective therapeutic strategies. This opportunity motivates the development of accurate imaging predictors of pCR and pathological non-response.

Diffuse optical imaging (DOI) technology, a potential candidate to address this clinical need, uses red and near-infrared (NIR) light (~600 to 1000 nm) to probe tissue absorption and scattering properties at depths up to several centimeters [21]. Absorption and scattering properties in this regime characterize tissue structure and function. Analogous to MRS and MRI, diffuse optical spectroscopic imaging (DOSI) is a specialized DOI technology that performs high-resolution spectroscopy from 650–1000nm where oxy- and deoxy-hemoglobin, water and lipid have prominent absorption features. These endogenous components vary significantly in abundance and molecular state between breast cancer and normal tissue [22–26] and unique cancer-specific absorption signatures not found in normal breast have been observed [27]. DOSI-measured tumor water concentration and water binding state were shown to scale with the Nottingham Bloom-Richardson histopathology score and appear to be proportional to tissue cellularity and extracellular matrix composition [22, 28]. Hemoglobin, water and bulk lipid components have been shown to be sensitive to microvasculature, cellular metabolism, angiogenesis, edema, hypoxia, and necrosis in several single-center studies and provide tumor contrast that can change significantly with the growth and regression of tumors [22, 29–35]. Quantitative, optical functional endpoints are easy to interpret and offer objective measures to predict therapeutic outcome and minimize patient toxicity. For instance, Tissue Optical Index (compound function of deoxy-hemoglobin, water and lipid tissue concentrations), which describes tissue metabolism, structure and cellularity, has been shown to be a promising imaging endpoint that significantly decreases by mid-therapy and can be used for predicting neoadjuvant

chemotherapy response [36]. Response to chemotherapy significantly correlated with a decrease in TOI by mid-therapy. The biological origins of this TOI signal change are NAC-induced reductions in tumor cellular density and edema (reduced water content), re-normalization of breast adipose displaced by the tumor (increased lipid fraction), and decreased levels of deoxyhemoglobin due a loss of metabolically active tumor cells. Any diffuse optical imaging instrument that uses the appropriate wavelength bands to retrieve hemoglobin, water and lipid information can calculate TOI. Because DOSI is a relatively inexpensive, portable, risk-free technology, it can be used frequently at the bedside, potentially creating new opportunities for patients to receive personalized treatment and for physicians to gain insight into response mechanisms. These features have been highlighted in several single-center studies and they motivated American College of Radiology Imaging Network (ACRIN) 6691, which was designed to evaluate whether quantitative DOSI measurements can be conducted in a prospective, multi-center trial setting to predict therapeutic response in breast cancer patients undergoing NAC. The primary aim was to evaluate whether the baseline to mid-therapy change of the DOSI-derived tissue optical index (TOI) could predict pCR. The secondary aims investigate the utility of additional DOSI measurements of tumor biochemical composition, obtained both at baseline and other time-points, for predicting pCR.

2. Materials and Methods

2.1. Subject eligibility and enrollment

Seven institutions were approved to enroll a total of 60 female breast cancer patients: Dartmouth Hitchcock Medical Center (Dartmouth), Massachusetts General Hospital (MGH), University of California Irvine (UCI), University of California San Francisco (UCSF), University of Pennsylvania (UPenn), Boston University (BU) and MD Anderson Cancer Center (MDACC). Enrollment began in June 2011 and completed in June 2013. All institutions activated concurrently, except MDACC and BU which joined the study in January and May 2013, respectively.

Eligible subjects were females age 18 years or older with biopsy-proven invasive breast cancer of at least 2 cm in the greatest dimension (as measured by palpation or standard breast imaging techniques), who planned to receive NAC followed by surgery. No restrictions were placed on menopausal status, tumor stage, or tumor subtype/pathology. For this study, the chemotherapy regimen was determined by the treating oncologist, and regimens containing at least one cytotoxic chemotherapeutic agent were required. Neoadjuvant hormonal therapy or other targeted agents alone in the absence of cytotoxic chemotherapy was not allowed. Potential subjects who received previous treatments, such as chemotherapy, endocrine therapy, radiation, or surgery (excluding breast augmentation) to the involved breast were excluded from the study. In addition, women who were pregnant or nursing were excluded. All subjects provided written informed consent. The HIPAA-compliant protocol and informed consent were approved by the American College of Radiology Institutional Review Board, the NCI Cancer Therapy Evaluation Program (CTEP), and each site’s Institutional Review Board.

2.2. DOSI – Instrumentation

DOSI measurements were performed with systems that combine frequency domain photon migration (FDPM) and broadband near-infrared (NIR, 650–1000 nm) spectroscopy for quantitative, model-based measurement of tissue absorption and scattering properties and recovery of tissue oxy-hemoglobin ($ctHbO_2$), deoxy-hemoglobin (ctHHb), water, and lipid. The full technical details of the system are described elsewhere [37]. Standardized procedures were developed for data collection and to monitor instrument performance. Three sets of three calibration measurements on two custom-fabricated solid breast-tissue simulating phantoms (Institut National d'Optique, Quebec, Canada and UC Irvine Beckman Laser Institute, CA, USA) and on one reflectance standard (SRS-99–020, Labsphere, Inc, NH, USA) were performed before, mid-way and after each subject measurement. The breast tissue simulating phantoms and reflectance standards used at all sites were identical. These measurements were used for determining instrument response-function, cross-calibration between instruments, and monitoring instrument performance over the duration of the study [38]. Dartmouth, MGH, UCI, UCSF, and UPenn used identical DOSI instruments. MDACC and BU, which joined the trial about 1.5 years after the first patient enrollment, used a smaller, portable version with equivalent features and performance to the original 5 DOSI instruments. The handheld DOSI probe that is scanned on the breast for data collection was identical for all instruments. A group of trainers from UCI, who developed the DOSI instruments, traveled to each site for initial instrument setup and training.

2.3. DOSI – Spectroscopy

The approach to DOSI data acquisition and analysis has been previously described [22], and is briefly summarized here. Concentrations of oxy-hemoglobin ($ctHbO_2$), deoxy-hemoglobin (ctHHb), water (ctH_2O), and bulk lipid were calculated by fitting a linear combination of their known molar extinction coefficient spectra to the tissue μ_a values derived from model-based fits of DOSI data [22]. From these quantities, the total blood volume ($THb = ctHHb + ctHbO_2$), percent oxygen saturation (StO_2) and tissue optical index (TOI) were calculated. The StO_2 is the ratio of $ctHbO_2$ to THb. TOI is defined as $TOI = ctHHb \times ctH_2O/lipid$. Prior single-center studies have shown that TOI can provide high tumor to normal (T/N) tissue contrast and that changes in T/N TOI are sensitive to chemotherapy response [22, 36]. Quantitative images of these local tissue concentrations and contrast function were formed on a generic 3D breast surface for visualization.

2.4. Imaging Procedures

DOSI scans were performed prior to the start of the chemotherapy treatment (baseline), 5 to 10 days after the first cycle (early-), at a change in chemotherapy regimens or mid-way through a single regimen protocol (mid-), and within 3 weeks after completion of the chemotherapy treatment but prior to surgery (post-therapy). The mid-therapy DOSI measurement was performed at least 5 days after the completion of the last cycle prior to the mid-point, and prior to the first cycle after the mid-point. Early- and post-therapy scans were optional as they were not required to analyze the primary aim.

DOSI measurements were performed using a standard protocol. Subjects were measured in a supine or reclining position. The DOSI probe was placed against the breast tissue, and

sequential measurements were recorded in a rectangular grid pattern using 10-mm spacing. Both breasts were specified to be measured at each visit. The dimension of the grids ranged from 7×7 to 15×16 cm^2 (i.e. 49 to 240 measurement locations). The grid size was chosen to fully encompass the tumor anatomical extent (by US or palpation) and to capture surrounding normal tissue. The grid on the non-cancerous contralateral breast (normal side) was mirrored from the grid on the cancerous breast (tumor side). An example of DOSI imaging grid locations and the resulting images is provided in Figure 1. For consecutive DOSI visits, individual static landmarks such as moles or freckles were recorded on a transparency sheet and provided a fixed reference to co-register the imaging grid at follow-up DOSI sessions. After initial processing performed centrally by the UCI/ACRIN core lab (see image analysis below), DOSI data from each session were plotted using grid coordinates and heat map functions in MATLAB. Linear interpolation was used to account for 10 mm spacing of grid points. The colored 2D maps were then overlaid on a 3D textured mesh of a realistic breast anatomic model with grid points drawn on it. The initial 3D image was obtained by using an X-box Kinect scanner for windows and accompanying software development kit (Microsoft, WA, USA). Colored heat maps obtained from MATLAB were warped and overlaid on the textured mesh using Photoshop CS6 Extended (Adobe, CA, USA) to create the final images.

2.5. Histopathological Assessment

Histopathological analysis of surgical specimens was performed locally by each institution's pathologist. One central pathologist (UCI core) then reviewed all pathological reports to assess individual tumor response. The binary determination of pathological complete (pCR) or non-complete (non-pCR) response was made based on evaluation of the pathology reports, and if needed, standard-of-care imaging reports. All determinations were made blinded to DOSI imaging data. Pathological complete response was standardized and defined as no residual of invasive disease present in the surgically resected tissue (breast and lymph nodes) as per FDA guidelines (http://www.fda.gov/downloads/drugs/guidancecomplianceregulatoryinformation/guidances/ucm305501.pdf). Non-pCR included both partial and non-responders. For the purposes of this report, only pCR status (0 or 1) was used to evaluate clinical outcome. Partial response characteristics will be further characterized in future analyses of secondary aims.

2.6. Image Analysis

A single analyst from UCI processed the de-identified raw DOSI data centralized from all participating institutions, and recovered the mean and standard deviation in tumor and normal tissue of all DOSI parameters. All DOSI data processing, including model-based fits to raw data, calculation of breast tissue composition, and image generation, was performed blinded with respect to clinical outcome on de-identified data by the UCI data core team. These processed data were transferred to the central ACRIN facility for further statistical analysis by the ACRIN Biostatistics Center. From the DOSI images, two regions of interest (ROI) representing tumor and normal tissue were defined using an automated algorithm. DOSI parameters were determined by calculating the mean of the measurement locations in each ROI. In this work, we focus on the tumor to normal ratio, which accounts for chemotherapy-induced changes in normal tissue.

As described in previous studies, the tumor ROI consisted of the full-width-at-half-maximum (FWHM) region around the baseline TOI tumor peak [36]. The DOSI measurement locations that had greater TOI values than a threshold equal to half the peak were included in the tumor ROI. In addition, a continuity rule was implemented to define the tumor ROI: any location calculated as part of the ROI but spatially disconnected (> 2cm away) was excluded from the ROI, and any location not meeting the threshold but surrounded by at least three other included points was incorporated. The tumor ROI size was fixed for all time-points, but the tumor ROI could be translated up to 2 cm at later time-points to account for a shift in tumor TOI enhancement (due to asymmetric tumor shrinkage or grid misplacement on the breast). This method was designed to capture the entire tumor region, but since the tumor size was longitudinally fixed, it overestimates the tumor extent at later time-points in responders.

The normal tissue ROI was selected in the contralateral breast to mirror the ipsilateral tumor ROI.

2.7. Statistical Methods

Summary statistics including the mean, standard deviation, median and range were computed for all DOSI markers. Logistic regression was used to model the association between percent change in tumor to normal (T/N) TOI ratio ($\%TOI_{TN}$) from baseline to mid-therapy and pathological response status (pCR vs. non-pCR). The resulting odds ratio and 95% CI were reported. In addition, a receiver operating characteristic (ROC) curve was derived for $\%TOI_{TN}$ with pathological response status as the reference standard. Area under the ROC curve (AUC) and the associated 95% confidence interval were computed empirically. If the lower limit of the 95% CI for AUC was at least 0.50, then the marker was considered capable of differentiating pCR vs. non-pCR.

To account for the heterogeneous cohort, the predictive power of $\%TOI_{TN}$ was evaluated further on two subsets of patients stratified by baseline tumor tissue oxygen saturation (StO_2), which is an optical parameter reflective of the tumor biophysical state. Tumor baseline StO_2 has been shown to be a promising predictor for pCR at early time-points [33, 39]. The median value of baseline StO_2 was used to stratify the subsets, with ROC curve and corresponding AUC reported for each subset. Evaluation of baseline StO_2 alone and in combination with midpoint $\%TOI_{TN}$ was a planned secondary aim of the study.

ACRIN 6691 was powered to detect an odds ratio of 3.0 using a two-sided hypothesis test, a type I error rate of 0.05, and 90% power (PASS 2008). The resulting sample size was determined to be 47 evaluable subjects. All tests were two-sided with p-value < 0.05 considered statistically significant. Statistical computations were done using SAS 9.3 (SAS Institution, Cary, NC) and R v3.1.0 (R project, http://www.r-project.com).

3. Results

3.1. Enrollment information

The target accrual was met with 60 subjects enrolled in ACRIN 6691. As depicted in Figure 2, three subjects withdrew from the study. An additional 12 subjects were not included in the

imaging analysis because of the following DOSI scan issues: mandatory baseline DOSI not performed (n = 1), baseline DOSI non-evaluable (n = 8), mandatory mid-therapy DOSI not performed (n = 3). A DOSI scan was considered non-evaluable in case of unrealistic physiological values, or incorrect instrument configuration. This decision was made on blinded, de-identified data using instrument calibration and raw data QC reports. Of the 45 eligible subjects with evaluable DOSI scans, one surgical pathology report after chemotherapy was not available. For another 10 subjects, the DOSI scan of the contralateral breast was not performed due to insufficient time during the measurement session to complete the normal side breast scan, which was required in this analysis for tumor to normal (T/N) values. The analysis therefore included 34 subjects with evaluable DOSI scans and available pathologic response data from 5 different institutions (Supplementary Table 1). Measurements at the two mandatory time-points to assess the primary aim, baseline and mid-therapy, were performed in 97% and 88% of all enrolled subjects, respectively (Supplementary Table 2). Despite being optional, measurements at early-therapy and post-therapy were performed in 73% and 82% of all enrolled subjects, respectively.

3.2. Subject and tumor characteristics

Table 1 presents the characteristics of all enrolled subjects (n = 60), and those subjects included in the analysis of the primary aim (n = 34). Among analyzed subjects, the average age was 48.4 ± 10.7 years (range 30–67 years), with 50% pre-menopausal, 3% peri-menopausal, and 47% post-menopausal. The racial distribution was 56% White, 24% Black, 12% Asian, and 9% of unknown race; 15% of analyzed subjects were of Hispanic or Latino ethnicity. Pre-chemotherapy tumor characteristics are also reported in Table 1. IDC accounted for approximately 85% of the tumors (with or without a DCIS component, and including 6% of cases mixed with an ILC component) in the analysis group. Notably, approximately 71% of the tumors in the analysis group were ER positive.

The chemotherapy protocols undergone by the subjects were not controlled in this study and, as a result, were highly heterogeneous. Treatments for all subjects were based on cytotoxic therapies. Targeted agents, such as Avastin (Bevacizumab) or Herceptin (Trastuzamab), could be used in combination of the cytotoxic agents. Hormonal therapies were not allowed. A total of 17 different chemotherapy protocols, including 12 different drugs, were administered in the 34 evaluable cases. HER2 status was known in 25/34 (74%) analyzable subjects. Trastuzamab was administered to 10/11 (91%) HER2 positive tumors, and Bevacizumab was administered to 1/2 (50%) triple negative tumors.

3.3. Pathologic outcome statistics

At surgery, 10 (29%) pathological complete responses (pCR) and 24 (71%) non-pCRs were included in the analysis group. A similar distribution of 15 (25%) pCRs was observed in all 60 enrolled subjects, with 5 (8%) not undergoing surgery/lost to follow-up.

3.4. DOSI during neoadjuvant chemotherapy

Figure 3 presents 2 typical examples of a pCR and a non-pCR measured using DOSI during NAC. The corresponding $\%TOI_{TN}$ is shown across NAC for both responses. Both subjects exhibited relatively high baseline TOI levels of ~3–4 at tumor and arealor regions. The pCR

subject demonstrated a greater $\%TOI_{TN}$ decrease at midpoint than the non-pCR subject (~46% and ~14%, respectively). Peak areolar TOI levels for subjects remained approximately the same throughout therapy.

3.5. Response Prediction – Tumor to Normal TOI change from baseline to mid-therapy

Among analyzable subjects the distribution of $\%TOI_{TN}$ from baseline to mid-therapy ranged from −82.4% to 320.8%, with a median of −36.2%. The corresponding mean (standard deviation) was −25.9% (67.2%). Figure 4 A) presents the distribution of $\%TOI_{TN}$ from baseline to mid-therapy by pathologic response category. On average, the pCR group exhibited a greater decrease in $\%TOI_{TN}$ than the non-pCR group; however, large variability occurred in $\%TOI_{TN}$ in the non-pCR group.

The protocol-planned logistic regression analysis demonstrated an odds ratio for pCR prediction of 1.4 (95% CI 0.7 to 2.9, p = 0.40) per standard deviation increase in $\%TOI_{TN}$. As strong evidence of model lack of fit existed using continuous $\%TOI_{TN}$, we explored using −40% to dichotomize the population for the purpose of logistic regression, which was approximately equal to the median $\%TOI_{TN}$ across all subjects. Patients who had a 40% or larger decrease in TOI_{TN} from baseline to mid-therapy were more likely to be complete responders than patients who experienced smaller decreases or increases, with an estimated odds ratio for pCR prediction of 4.7 (95% CI 0.9 to 23.0, p = 0.059), see Table 2. The ROC AUC for pCR using $\%TOI_{TN}$ was 0.60 (95% CI 0.39 to 0.81), suggesting this marker does not exhibit good discriminatory ability for pCR in the entire cohort (Figure 5 A).

In the subset analysis, subjects were further stratified using the median tumor StO_2 at baseline (76.9%) as another binary marker. Note that this median baseline tumor StO_2 is similar to the threshold value reported by Ueda et al. [39], 76.7%, which has been shown to correlate with NAC response. Figure 4 B) and C) show the distributions of $\%TOI_{TN}$ from baseline to mid-therapy by pathologic response category in each subset. While $\%TOI_{TN}$ in patients with low baseline tumor StO_2 did not correlate with pathologic response, a large decrease in $\%TOI_{TN}$ from baseline to mid-therapy in patients with high baseline tumor StO_2 was associated with pathologic complete response. For 17 subjects with baseline StO_2 greater than 76.9%, AUC was 0.83 (95% CI 0.63 to 1.00, Figure 5 C). These subjects were more likely to be complete responders than patients who experienced smaller decreases or increases, with an estimated odds ratio for pCR prediction of 16.5 (95% CI 1.1 to 250.2 p = 0.043), see Table 2.

Discussion

ACRIN 6691 is the first multi-center breast imaging trial utilizing DOSI technology. As its primary aim, the trial was designed to evaluate whether $\%TOI_{TN}$ from baseline to mid-therapy was predictive of the final pathologic response of breast cancer during neoadjuvant chemotherapy. DOSI measurements were successfully performed longitudinally throughout NAC at 6 different institutions across the USA.

Standard-of-care NAC response is currently assessed using changes in anatomical tumor size. However, anatomical assessment has been shown to be an unreliable metric of

pathological response and arises after a measurable change in functional characteristics [7, 19, 20]. Functional imaging techniques, such as dynamic contrast enhanced (DCE) MRI and PET have shown better predictive value than anatomical imaging methods [10, 40], but they are costly, involve lengthy scan times, and require injection of a contrast agent, which limit availability and measurement frequency. DOSI is a portable, non-invasive intrinsic-signal technique that monitors functional tumor response during NAC and may predict early clinical outcome. Frequent longitudinal DOSI measurements were first reported to reveal dynamic tumor physiology [41], and validated the TOI endpoint in a single-site 34-subject study by showing $\%TOI_{TN}$ is significantly different at mid-therapy for pCR vs. non-pCR NAC patients [36]. Additional studies by several groups have confirmed the sensitivity of diffuse optical methods to breast cancer NAC response using both baseline and dynamic response measures [30–32, 42–48]. Although these studies were completed with different instruments and NAC protocols, their common findings indicate that tumor cell metabolism and vascularity are significantly altered during chemotherapy and optical methods are sensitive to several markers of these changes. For example, NAC-induced cellular damage alters tumor oxygen consumption and lowers tumor ctHHb; vascular damage causes a decrease in tumor $ctHbO_2$, and progressive loss of cellularity and edema results in a decrease in tumor water content.

The current multi-center clinical trial was devised to evaluate NAC response using a single, standardized DOSI platform and TOI endpoint. Extensive validation and performance assessment features were built into the study in order to evaluate the potential use of DOSI technologies in patient management. As expected, we observed that the 10 subjects achieving pCR exhibited dramatic decreases in TOI_{TN} from baseline to mid-therapy. However, while many non-pCR tumors exhibited lesser TOI_{TN} changes, significant TOI_{TN} decreases were, nonetheless, observed in some of the non-pCR tumors. Although a previous single site study using identical DOSI technology showed $\%TOI_{TN}$ was significantly different at mid-therapy for pCR vs. non-pCR patients [36], the variability among non-pCR subjects limited the ability of $\%TOI_{TN}$ to discriminate between pCR and non-pCR in the multi-center setting. This outcome may be due to factors that were not controlled for in the current study including diverse tumor biology, widely varying chemotherapy regimens, and the fact that pathological response is performed on a microscopic level. Nevertheless, pCR has been recognized by the FDA as a validated endpoint for evaluating drug efficacy and it is a surrogate for 5-year survival. The pCR endpoint has been used in a similar manner to test and validate several imaging technologies including PET, MRI, and ultrasound for monitoring and predicting NAC response. Several previous ACRIN NAC trials of experimental imaging endpoints have been based on pCR including ACRIN 6657 for MRI and ACRIN 6688 for PET.

The importance of studying individual NAC treatment response is supported by recent work, which suggests that pCR may not be correlated with disease-free survival in certain NAC agents [49]. The $\%TOI_{TN}$ variability we observe is primarily a result of the diverse responses observed in the non-pCR group, which includes subjects who have a significant tumor burden, as well as subjects with only small clusters of remaining tumor cells. A more refined clinical assessment of the non-pCR group using a continuously variable endpoint, such as the residual cancer burden [50] or the Miller-Payer system [51], could lead to a

better understanding of the non-pCR TOI_{TN} changes, and to a better separation of $\%TOI_{TN}$ between response groups. The total number of non-pCR subjects is too small, however, to conduct such an examination in this study. In addition, 17 out of the 34 evaluable tumors were involved to some degree in the areolar complex. In pre-menopausal females, the areolar region is metabolically active, and, in some cases, it has been shown to exhibit NAC induced changes in metabolism measured using DOSI [52]. Our results suggest that there is a trend toward differential performance of $\%TOI_{TN}$ in areolar vs. non-areolar tumors, with better discriminatory ability in non-areolar tumors [ROC AUC=0.52 95% CI (0.18, 0.85) vs. 0.70 95% CI (0.43, 0.97)]; however, given the small sample size in each subset (N=17), there was large variability in the point estimates and this difference was not statistically significant (p=0.41). A larger sample size would be needed to confirm this trend. Nevertheless, the large magnitude of tumor changes observed in non-pCR subjects with retroareolar tumors may, in part, be due to the response of metabolically active areolar breast tissue combined with adjacent involved tumor. These factors impact the magnitude of the tumor response measured using DOSI and they underscore the importance of controlling the environment (tumor type, chemotherapy protocol, etc.) in order to optimally predict therapeutic response.

Hypoxia, characterized in part by low StO_2 levels, is often present in locally advanced breast tumors due to a combination of abnormal tumor microvessels, elevated tumor metabolism, and high tumor osmotic pressures [53]. Previous studies have shown that pre-chemotherapy tumor oxygen saturation [39] and total hemoglobin [48] may be good prognostic tools for predicting therapeutic outcome. Here, the data also suggest that tumor oxygen saturation plays an important role in predicting pCR. Improved pCR prediction was observed when performing the primary analysis on tumors with baseline tumor oxygen saturation greater than the median value (77%). This prediction was not possible in subjects with baseline tumor oxygen saturation <77%. These results suggest that baseline tumor oxygen saturation may be important in stratifying the population for evaluating DOSI response. Overall, baseline tumor StO_2 appears to be an important imaging biomarker that can be used in combination with dynamic changes to predict clinical outcome. However, the underlying origin of this response is not yet known. The predictive power of the $\%TOI_{TN}$ dynamic response may be restricted to well-oxygenated tumors because of technical reasons related to DOSI, or because of the biological advantage of oxygenation. Establishing threshold criteria for baseline DOSI measurements could play an important role in interpreting the tumor dynamic response and, ultimately, employing DOSI to improve patient outcome. Establishing predictive thresholds is expected to be sensitive to both the technology employed and the patient population. Their practical use in clinical management and outcome prediction will depend on whether baseline parameters can be clearly defined both within and across technology platforms and this should be the focus of future studies.

In order to assess the uniqueness of DOSI endpoints, our results were evaluated for the possible confounders of pre-treatment molecular subtype and tumor size. Both have been used previously to stratify patient therapeutic response predictions [54, 55]. No association was found between baseline tumor oxygen saturation and molecular subtype in the 31 out of 34 evaluable patients where these data were available (p=0.41 for ER status and p=1.0 for PR status from Fisher’s exact test). Low correlation also occurred between baseline tumor

oxygen saturation and tumor size (measured by ultrasound, US) in the 19 out of the 34 patients where baseline tumor size was available (Spearman correlation = −0.39, p=0.10).

Studies have shown that diffuse optical techniques are sensitive to breast tissue composition changes during the menstrual cycle [56–58]. To account for these biological changes and for chemotherapy-induced changes in normal tissue, the tumor-to-normal ratio was reported. This resulted in ten subjects excluded from the analysis due to the absence of contralateral tissue measurement. As part of the secondary aims, changes of tumor values rather than tumor to normal ratio will be reported in future analysis. However, the preliminary results were not as promising as the ratiometric analysis.

Study limitations

Important study limitations were the diversity of the patient population, heterogeneity of tumor molecular subtypes, and lack of standardized chemotherapy regimens. In addition, the adequate sample size was determined to be 47 subjects; however, only 34 out of the 60 enrolled cases were assessed as analyzable. Since this study was the first multicenter trial that tested longitudinal DOSI measurements during NAC, much effort was focused on instrument and procedure standardization. Each instrument was fabricated and tested at UC Irvine using a common set of tissue-simulating phantoms before delivery to the study site. These phantoms were used to assess instrument performance throughout study. Preliminary analysis demonstrated <1% variability in broadband DOSI over 1 hour (typical patient measurement time-frame), <5% over 4 months (typical chemotherapy measurement time-frame), and <6% over the 2-year study duration. Although operators at all institutions were trained to perform standard measurement procedures, clinical DOSI data were in general of poor quality for the first few subjects. Data quality improved with more practice and feedback, nevertheless, the number of non-evaluable cases was primarily due to operator error that led to incorrect instrument settings and poor data quality, as well as clinical work-flow time pressures that resulted in lack of normal side data on several subjects. Also, a large disparity in subject enrollment occurred across institutions: UCI and MDACC enrolled about two thirds of the subjects, while MGH and UCSF enrolled a total of 3 and 2 subjects, respectively. As the technique and instrument become more standardized, and through the experience gained with this study, ease-of-use is expected to improve, and the number of non-evaluable cases is expected to decline in future multi-center studies. Finally, tumor dimensions by ultrasound matching the DOSI scan date at +/− 2 weeks (at baseline and mid-therapy) were available for only 12 subjects. Of those, only 2 were pCR, limiting our ability to make a DOSI-Ultrasound comparison.

Future Analysis

Analysis of ACRIN 6691 secondary aims is ongoing, including examining other DOSI dynamic response endpoints, baseline parameters, and molecular subtype. Further analyses will also explore the development of new indices to report tumor changes. Finally, the tumor ROI used in this study was obtained with an algorithm based on the full-width-at-half-maximum (FWHM) around the baseline (pre-chemotherapy) TOI peak. While some groups have explored the impact of different ROIs on NAC prediction of diffuse optical imaging

[31, 32], currently no standardized method exists to determine tumor ROI in DOSI data. The effect of ROI choice will, therefore, be examined in future work.

Conclusion

As an experimental cancer imaging technology, Diffuse Optical Spectroscopic Imaging (DOSI) has been tested for the first time in ACRIN 6691, an independently-executed, prospective multi-center trial of breast cancer neoadjuvant chemotherapy (NAC). The results demonstrated that although a range of responses to NAC were observed in this heterogeneous patient population, subjects exhibiting a greater drop in $\%TOI_{TN}$ from baseline to mid-therapy were more likely to have a pathologic complete response (pCR) to NAC. While this change alone was not a strong predictor of clinical outcome for the full patient population, its performance was substantially improved when patients were stratified according to baseline tumor oxygen saturation levels. Importantly, the same dynamic $\%TOI_{TN}$ change was unable to predict pCR in subjects with baseline tumor oxygen saturation lower than the median value. This finding suggests that stratification using baseline tumor properties, especially oxygenation, can be used to improve DOSI therapy response predictions for individual subjects, particularly among diverse patient populations and NAC treatment strategies.

Supplementary Material

Refer to Web version on PubMed Central for supplementary material.

Acknowledgments

Financial Support: This research was supported by the American College of Radiology Imaging Network, ACRIN, which receives funding from the National Cancer Institute (NCI) through the grants U01 CA079778 and U01 CA080098 (Clinical trial information: NCT01217385), the National Institute of Biomedical Imaging and Bioengineering (P41EB015890), the National Cancer Institute (R01CA142989, U54CA136400) and the Chao Family Comprehensive Cancer Center (P30CA62203), and programmatic support from the Arnold and Mabel Beckman Foundation.

The authors thank the entire ACRIN staff for their generous support in completing this study, including Donna Hartfeil, Sharon Mallet, and Dunstan Horng; UCI coordinators Montana Compton, Erin Sullivan, and Jennifer Ehren; UCI engineers Amanda Durkin and Brian Hill; clinical coordinators at all sites, and the patients who generously volunteered their time for this study.

References

1. Gralow JR, Zujewski JA, Winer E. Preoperative therapy in invasive breast cancer: reviewing the state of the science and exploring new research directions. Journal of Clinical Oncology. 2008; 26(5):696–697. [PubMed: 18258975]
2. Sledge GW, et al. Past, Present, and Future Challenges in Breast Cancer Treatment. Journal of Clinical Oncology. 2014; 32(19):1979–1986. [PubMed: 24888802]
3. Esserman LJ, et al. Chemotherapy response and recurrence-free survival in neoadjuvant breast cancer depends on biomarker profiles: results from the I-SPY 1 TRIAL (CALGB 150007/150012; ACRIN 6657). Breast Cancer Research and Treatment. 2012; 132(3):1049–1062. [PubMed: 22198468]
4. Rastogi P, et al. Preoperative chemotherapy: updates of national surgical adjuvant breast and bowel project protocols B-18 and B-27. Journal of Clinical Oncology. 2008; 26(5):778–785. [PubMed: 18258986]

5. FDA. Available from: http://www.fda.gov/downloads/drugs/guidancecomplianceregulatoryinformation/guidances/ucm305501.pdf
6. Yeh E, et al. Prospective comparison of mammography, sonography, and MRI in patients undergoing neoadjuvant chemotherapy for palpable breast cancer. American Journal of Roentgenology. 2005; 184(3):868–877. [PubMed: 15728611]
7. Vinnicombe SJ, et al. Primary breast cancer: mammographic changes after neoadjuvant chemotherapy, with pathologic correlation. Radiology. 1996; 198(2):333–340. [PubMed: 8596827]
8. Helvie MA, et al. Locally advanced breast carcinoma: accuracy of mammography versus clinical examination in the prediction of residual disease after chemotherapy. Radiology. 1996; 198(2):327–332. [PubMed: 8596826]
9. Feldman LD, et al. Pathological assessment of response to induction chemotherapy in breast cancer. Cancer Research. 1986; 46(5):2578–2581. [PubMed: 3697997]
10. Hylton NM, et al. Locally advanced breast cancer: MR imaging for prediction of response to neoadjuvant chemotherapy—results from ACRIN 6657/I-SPY TRIAL. Radiology. 2012; 263(3): 663–672. [PubMed: 22623692]
11. Chenevert TL, et al. Diffusion magnetic resonance imaging: an early surrogate marker of therapeutic efficacy in brain tumors. Journal of the National Cancer Institute. 2000; 92(24):2029–2036. [PubMed: 11121466]
12. Meisamy S, et al. Neoadjuvant Chemotherapy of Locally Advanced Breast Cancer: Predicting Response with in Vivo 1H MR Spectroscopy—A Pilot Study at 4 T 1. Radiology. 2004; 233(2): 424–431. [PubMed: 15516615]
13. Mankoff DA, et al. Changes in blood flow and metabolism in locally advanced breast cancer treated with neoadjuvant chemotherapy. Journal of Nuclear Medicine. 2003; 44(11):1806–1814. [PubMed: 14602864]
14. McDermott GM, et al. Monitoring primary breast cancer throughout chemotherapy using FDG-PET. Breast Cancer Research and Treatment. 2007; 102(1):75–84. [PubMed: 16897427]
15. Kostakoglu L, et al. A Phase II Study of 3′-Deoxy-3′-18F-Fluorothymidine PET in the Assessment of Early Response of Breast Cancer to Neoadjuvant Chemotherapy: Results from ACRIN 6688. J Nucl Med. 2015; 56(11):1681–9. [PubMed: 26359256]
16. Bozzetti C, et al. Evaluation of HER-2/neu amplification and other biological markers as predictors of response to neoadjuvant anthracycline-based chemotherapy in primary breast cancer: the role of anthracycline dose intensity. American journal of clinical oncology. 2006; 29(2):171–177. [PubMed: 16601438]
17. Burcombe R, et al. Evaluation of Ki-67 proliferation and apoptotic index before, during and after neoadjuvant chemotherapy for primary breast cancer. Breast Cancer Res. 2006; 8(3):31–33.
18. Dose-Schwarz J, et al. Assessment of residual tumour by FDG-PET: conventional imaging and clinical examination following primary chemotherapy of large and locally advanced breast cancer. Br J Cancer. 2009; 102(1):35–41. [PubMed: 19920815]
19. Symmans WF, et al. Paclitaxel-induced apoptosis and mitotic arrest assessed by serial fine-needle aspiration: implications for early prediction of breast cancer response to neoadjuvant treatment. Clinical Cancer Research. 2000; 6(12):4610–4617. [PubMed: 11156210]
20. Archer C, et al. Early changes in apoptosis and proliferation following primary chemotherapy for breast cancer. British Journal of Cancer. 2003; 89(6):1035–1041. [PubMed: 12966422]
21. O'Sullivan TD, et al. Diffuse optical imaging using spatially and temporally modulated light. Journal of Biomedical Optics. 2012; 17(7):0713111–07131114.
22. Cerussi A, et al. In vivo absorption, scattering, and physiologic properties of 58 malignant breast tumors determined by broadband diffuse optical spectroscopy. Journal of Biomedical Optics. 2006; 11(4):044005–044005. [PubMed: 16965162]
23. Pogue BW, et al. Near-infrared characterization of breast tumors in vivo using spectrally-constrained reconstruction. Technology in Cancer Research & Treatment. 2005; 4(5)
24. Spinelli L, et al. Characterization of female breast lesions from multi-wavelength time-resolved optical mammography. Physics in Medicine and Biology. 2005; 50(11):2489–2502. [PubMed: 15901950]

25. Taroni P, et al. Clinical trial of time-resolved scanning optical mammography at 4 wavelengths between 683 and 975 nm. Journal of Biomedical Optics. 2004; 9(3):464–473. [PubMed: 15189083]
26. Wang J, et al. In vivo quantitative imaging of normal and cancerous breast tissue using broadband diffuse optical tomography. Med Phys. 2010; 37:3715–3724. [PubMed: 20831079]
27. Kukreti S, et al. Intrinsic tumor biomarkers revealed by novel double-differential spectroscopic analysis of near-infrared spectra. J Biomed Opt. 2007; 12:020509. [PubMed: 17477706]
28. Chung SH, et al. In vivo water state measurements in breast cancer using broadband diffuse optical spectroscopy. Physics in Medicine and Biology. 2008; 53(23):6713–6727. [PubMed: 18997265]
29. Cerussi A, et al. Predicting response to breast cancer neoadjuvant chemotherapy using diffuse optical spectroscopy. Proceedings of the National Academy of Sciences of the United States of America. 2007; 104(10):4014–4019. [PubMed: 17360469]
30. Choe R, et al. Diffuse optical tomography of breast cancer during neoadjuvant chemotherapy: A case study with comparison to MRI. Medical Physics. 2005; 32(4):1128–1139. [PubMed: 15895597]
31. Falou O, et al. Diffuse optical spectroscopy evaluation of treatment response in women with locally advanced breast cancer receiving neoadjuvant chemotherapy. Translational oncology. 2012; 5(4): 238. [PubMed: 22937175]
32. Jiang S, et al. Evaluation of Breast Tumor Response to Neoadjuvant Chemotherapy with Tomographic Diffuse Optical Spectroscopy: Case Studies of Tumor Region-of-Interest Changes. Radiology. 2009; 252(2):551–560. [PubMed: 19508985]
33. Roblyer D, et al. Optical imaging of breast cancer oxyhemoglobin flare correlates with neoadjuvant chemotherapy response one day after starting treatment. Proc Natl Acad Sci USA. 2011; 108:14626–14631. [PubMed: 21852577]
34. Soliman H, et al. Functional Imaging Using Diffuse Optical Spectroscopy of Neoadjuvant Chemotherapy Response in Women with Locally Advanced Breast Cancer. Clinical Cancer Research. 2010; 16(9):2605–2614. [PubMed: 20406836]
35. Zhu Q, et al. Noninvasive monitoring of breast cancer during neoadjuvant chemotherapy using optical tomography with ultrasound localization. neoplasia. 2008; 10(10):1028–1040. [PubMed: 18813360]
36. Cerussi AE, et al. Diffuse optical spectroscopic imaging correlates with final pathological response in breast cancer neoadjuvant chemotherapy. Philosophical Transactions of the Royal Society A: Mathematical, Physical and Engineering Sciences. 2011; 369(1955):4512–4530.
37. Bevilacqua F, et al. Broadband absorption spectroscopy in turbid media by combined frequency-domain and steady-state methods. Appl Optics. 2000; 39:6498–6507.
38. Cerussi A, et al. Quality control and assurance for validation of DOS/I measurements. 2010:756703–756703.
39. Ueda S, et al. Baseline tumor oxygen saturation correlates with a pathologic complete response in breast cancer patients undergoing neoadjuvant chemotherapy. Cancer Research. 2012; 72(17): 4318–4328. [PubMed: 22777823]
40. Kurland BF, et al. Feasibility study of FDG PET as an indicator of early response to aromatase inhibitors and trastuzumab in a heterogeneous group of breast cancer patients. EJNMMI research. 2012; 2(1):1–9. [PubMed: 22251281]
41. Jakubowski DB, et al. Monitoring neoadjuvant chemotherapy in breast cancer using quantitative diffuse optical spectroscopy: a case study. Journal of Biomedical Optics. 2004; 9(1):230–238. [PubMed: 14715078]
42. Carp, S., et al. Biomedical Optics. Optical Society of America; 2012. Neoadjuvant Chemotherapy Monitoring using Dynamic Breast Compression Imaging.
43. Enfield L, et al. Monitoring the response to neoadjuvant hormone therapy for locally advanced breast cancer using three-dimensional time-resolved optical mammography. Journal of Biomedical Optics. 2013; 18(5):056012–056012.
44. Jiang S, et al. Predicting breast tumor response to neoadjuvant chemotherapy with Diffuse Optical Spectroscopic Tomography prior to treatment. Clinical Cancer Research. 2014; 20(23):6006–6015. [PubMed: 25294916]

45. Pakalniskis MG, et al. Tumor angiogenesis change estimated by using diffuse optical spectroscopic tomography: demonstrated correlation in women undergoing neoadjuvant chemotherapy for invasive breast cancer. Radiology. 2011; 259(2):365–374. [PubMed: 21406632]
46. Schaafsma BE, et al. Optical mammography using diffuse optical spectroscopy for monitoring tumor response to neoadjuvant chemotherapy in women with locally advanced breast cancer. Clinical Cancer Research. 2015; 21(3):577–584. [PubMed: 25473002]
47. Xu C, et al. Ultrasound-Guided Diffuse Optical Tomography for Predicting and Monitoring Neoadjuvant Chemotherapy of Breast Cancers: Recent Progress. Ultrason Imaging. 2015; 16 0161734615580280.
48. Zhu Q, et al. Pathologic response prediction to neoadjuvant chemotherapy utilizing pretreatment near-infrared imaging parameters and tumor pathologic criteria. Breast Cancer Research. 2014; 16(5):456. [PubMed: 25349073]
49. Berruti A, et al. Pathologic Complete Response As a Potential Surrogate for the Clinical Outcome in Patients With Breast Cancer After Neoadjuvant Therapy: A Meta-Regression of 29 Randomized Prospective Studies. Journal of Clinical Oncology. 2014; 32(34):3883–3891. [PubMed: 25349292]
50. Symmans WF, et al. Measurement of residual breast cancer burden to predict survival after Neoadjuvant chemotherapy. Journal of Clinical Oncology. 2007; 25:4414–4422. [PubMed: 17785706]
51. Ogston KN, et al. A new histological grading system to assess response of breast cancers to primary chemotherapy: prognostic significance and survival. The Breast. 2003; 12(5):320–327. [PubMed: 14659147]
52. O'Sullivan T, et al. Optical imaging correlates with magnetic resonance imaging breast density and reveals composition changes during neoadjuvant chemotherapy. Breast Cancer Research. 2013; 15(1):R14. [PubMed: 23433249]
53. Vaupel P, Briest S, Höckel M. Hypoxia in Breast Cancer: Pathogenesis, Characterization and Biological/Therapeutic Implications Hypoxie beim Mammakarzinom: Pathogenese, Charakterisierung und biologische/therapeutische Konsequenzen. Wiener Medizinische Wochenschrift. 2002; 152(13–14):334–342. [PubMed: 12168517]
54. Lips E, et al. Neoadjuvant chemotherapy in ER+ HER2− breast cancer: response prediction based on immunohistochemical and molecular characteristics. Breast Cancer Research and Treatment. 2012; 131(3):827–836. [PubMed: 21472434]
55. Song I-H, Lee HJ, Gong G. Pathologic response pattern of breast cancer after neoadjuvant chemotherapy: its correlation with molecular subtypes. Cancer Research. 2014; 74(19 Supplement):1880–1880.
56. Shah N, et al. Noninvasive functional optical spectroscopy of human breast tissue. Proceedings of the National Academy of Sciences of the United States of America. 2001; 98(8):4420–4425. [PubMed: 11287650]
57. Pogue BW, et al. Characterization of hemoglobin, water, and NIR scattering in breast tissue: Analysis of intersubject variability and menstrual cycle changes. Journal of Biomedical Optics. 2004; 9(3):541–552. [PubMed: 15189092]
58. Cubeddu R, et al. Effects of the menstrual cycle on the red and near-infrared optical properties of the human breast. Photochemistry and Photobiology. 2000; 72(3):383–391. [PubMed: 10989610]

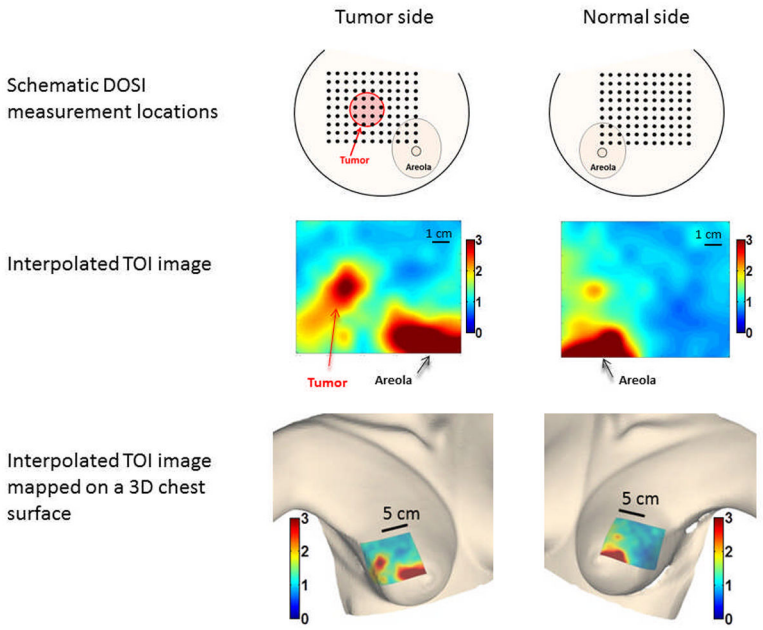

Figure 1.
Example of DOSI measurement grids and the corresponding TOI images (Subject 6691-21).

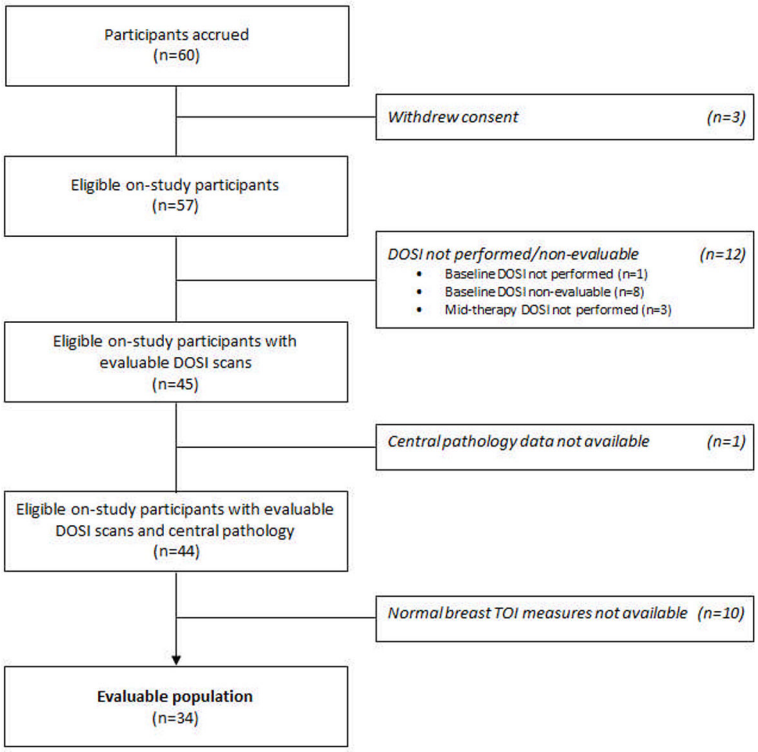

Figure 2.
Enrollment to analysis flowchart

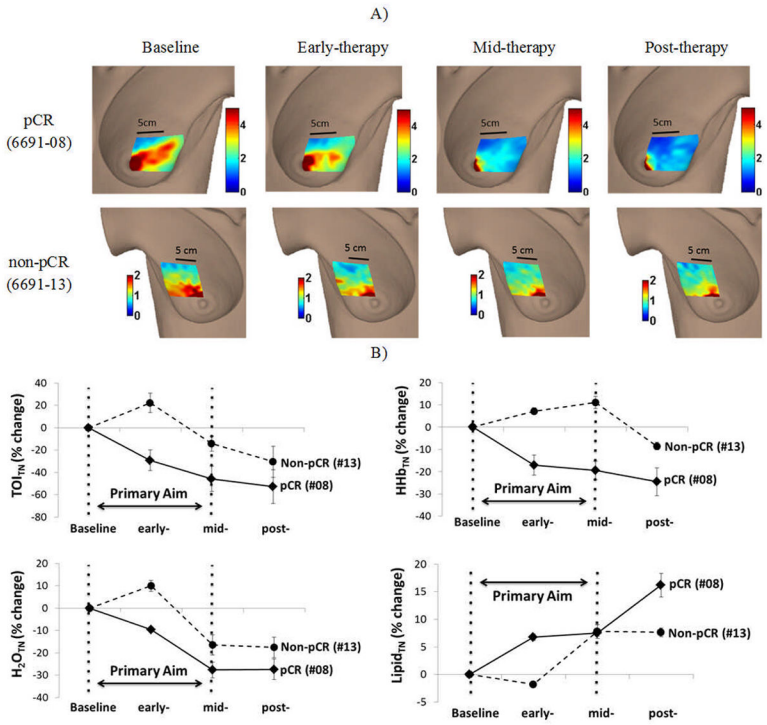

Figure 3.

DOSI Images throughout NAC for a pCR (6691-08) and a non-pCR (6691-13) subject. Scale bar illustrates Tissue Optical Index (TOI) values. B) Percent change in TOI_{TN}, HHb_{TN}, H_2O_{TN}, $Lipid_{TN}$ from baseline for both subjects. Error bars represent the SD of multiple measurement locations defined by the ROI for each subject (25 and 28 locations for 6691-08 and 6691-13, respectively).

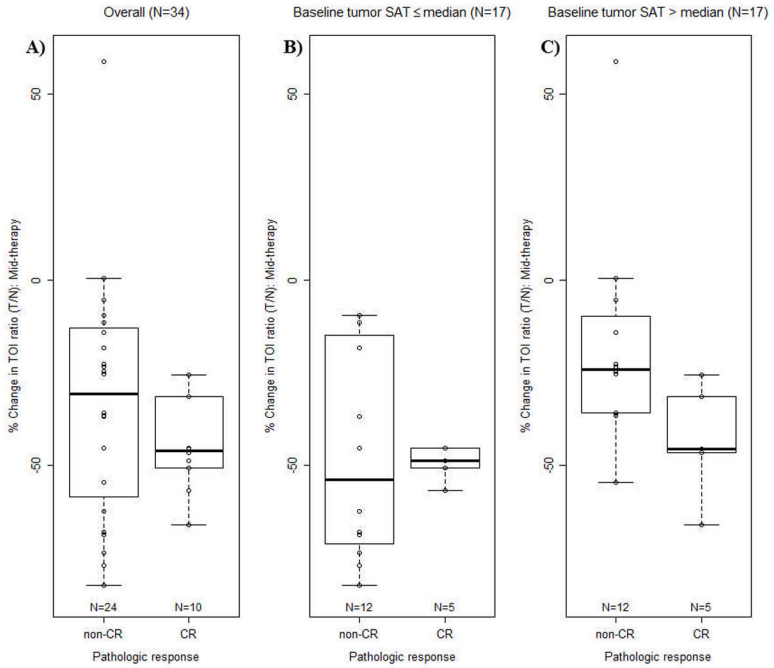

Figure 4.

Boxplot of percent change from baseline to mid-therapy in TOI_{TN} ($\%TOI_{TN}$) by final pathologic status, dichotomized as pCR vs. non-pCR. A) in the overall evaluable dataset; B) in the subset of evaluable cases with baseline tumor oxygenation lower than the median value; C) in the subset of evaluable cases with baseline tumor oxygenation greater than the median value.

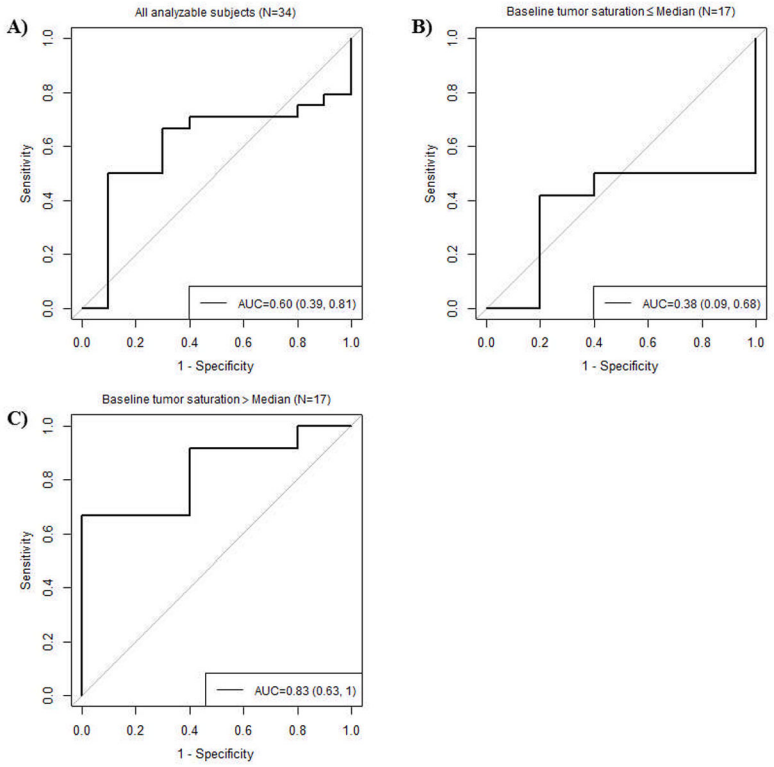

Figure 5.

ROC curves for pathologic complete response using percent change from baseline to mid-therapy in TOI_{TN} ($\%TOI_{TN}$) A) in the overall evaluable dataset, B) in the subset of evaluable cases with baseline tumor saturation lower than the median value, C) in the subset of evaluable cases with baseline tumor saturation greater than the median value. The reference standard is coded as follows: 0=pCR and 1=Non-pCR.

Table 1

Subject and tumor characteristics from initial pathology - Data are numbers of subjects, with percentages in parentheses.

	Analysis group N=34	All enrolled subjects N=60
Age, years		
Mean ± Std Dev (Range)	48.4 ± 10.7 (30–67)	48.9 ± 11.0 (28–69)
Menopausal status, n (%)		
Pre-	17 (50)	29 (48)
Peri-	1 (3)	4 (7)
Post-	16 (47)	26 (43)
Unknown	0 (0)	1 (2)
Race, n (%)		
White	19 (56)	37 (62)
Black/African-American	8 (24)	12 (20)
Asian	4 (12)	7 (12)
Native Hawaiian/Pacific Islander	0 (0)	1 (2)
Unknown	3 (9)	3 (5)
Ethnicity, n (%)		
Hispanic/Latino	5 (15)	7 (12)
Non-Hispanic/Latino	29 (85)	53 (88)
Histologic findings, n (%)		
IDC	16 (47%)	34 (57%)
ILC	3 (9%)	3 (5%)
DCIS/IDC	11 (32%)	16 (27%)
IDC/ILC	2 (6%)	2 (3%)
Other/Not available	2 (6%)	5 (8%)
ER status, n (%)		
Positive	24 (71%)	41 (68%)
Negative	7 (21%)	13 (22%)
Unknown	3 (9%)	5 (8%)
Not available	0 (0%)	1 (2%)
PR status, n (%)		
Positive	19 (56%)	34 (57%)
Negative	12 (35%)	20 (33%)
Unknown	3 (9%)	5 (8%)
Not available	0 (0%)	1 (2%)
Ki67 status, n (%)	17 (50%)	23 (38%)
Positive	2 (6%)	3 (5%)

	Analysis group N=34	All enrolled subjects N=60
Negative	15 (44%)	33 (55%)
Unknown	0 (0%)	1 (2%)
Not available		
Her2 status, n (%)		
0	4 (12%)	9 (15%)
1	8 (24%)	14 (23%)
2	8 (24%)	12 (20%)
3	4 (12%)	6 (10%)
Unknown/Not available	10 (29%)	19 (32%)
Fish status, n (%)		
Amplified	7 (21%)	9 (15%)
Nor Amplified	14 (41%)	29 (48%)
Unknown/Not available	13 (38%)	22 (37%)
Areolar tumor, n (%)		
Areolar tumor	17 (50%)	31 (52%)
Non-areolar tumor	17 (50%)	27 (45%)
N/A (DOSI not performed)	0 (0%)	2 (3%)

Table 2

Summary of odds ratios and significance for predicting pCR from logistic regression using percent change from baseline to mid-therapy in TOI_{TN} ($\%TOI_{TN}$). A) $\%TOI_{TN}$ dichotomized at −40%, B) $\%TOI_{TN}$ dichotomized at −40% for the subset of evaluable subjects with baseline tumor StO_2 > 76.9%. (i.e. population median).

DOSI endpoint binary marker	Number of subjects	Odds ratio (95% CI)	P-value
A) % TOI_{TN} ≤ −40%	34	4.7 (0.9, −23.0)	0.059
B) % TOI_{TN} ≤ −40% and baseline StO_2 >76.9%	17	16.5 (1.1, 250.2)	0.043